

## SWITCHABLE DISTANCE-BASED IMPEDANCE MATCHING NETWORKS FOR A TUNABLE HF SYSTEM

W.-S. Lee, H. L. Lee, K.-S. Oh<sup>\*</sup>, and J.-W. Yu

Department of Electrical Engineering, KAIST, 291 Daehak-ro, Yuseong-gu, Daejeon 305-701, Korea

**Abstract**—Distance-based impedance matching networks for a tunable high frequency (HF) system are presented in this paper for the improved performance. The transmitting antenna for a HF system with an operating frequency of 13.56 MHz consists of a two-turn loop and three channel impedance matching networks corresponding to the distance of the receiving antenna. Each impedance matching network maximizes the system performance such as uniform power efficiency and reading range at specific distance between a transmitting and a receiving antenna. By controlling the distance-based matching networks, the power efficiency of the proposed antenna improves by up to 89% compared to the conventional antenna system with the fixed matching (FM) condition for distances, and the reliable reading range according to the impedance matching conditions is also increased. The proposed technique is applicable for near field communication (NFC), radio frequency identification (RFID), or wireless power transfer (WPT) devices.

### 1. INTRODUCTION

With the development of mobile devices such as smart phones, wireless pads, and laptops, data and voice communications become more prevalent. Furthermore, the efficiency of RF systems is vital to wireless communications, and becomes even more critical when the antenna efficiency is changed by the neighboring environmental factors [1–5].

In particular, the antenna efficiency is highly sensitive in NFC or HF RFID systems because it is related to the coupling factor proportional to the distance between the transmitting and receiving

---

*Received 12 April 2012, Accepted 3 May 2012, Scheduled 14 May 2012*

<sup>\*</sup> Corresponding author: Kyoung-Sub Oh (ksfaraday@msn.com).

antennas [6–9]. Also, good impedance matching for efficient power transfer is essential for wireless power transfer technology since high  $Q$  resonant coils are widely used [10–15].

By reducing the mismatch in the RF front end systems through properly used impedance matching circuits, the transfer power efficiency or reading range is improved so that high quality communication can be achieved. Since the impedances of the reactive components in the matching circuits are frequency dependent, the impedance can only be perfectly matched at a single operating frequency or a limited band of frequencies. Therefore, tunable impedance matching networks can provide an advantage over fixed impedance matching networks by controlling lumped elements that can be optimally tuned for desired frequencies to overcome any potential impedance variations.

Due to the complicated nature [9,16] of manual impedance matching, an adaptive impedance matching module and control algorithms [17,18] that find the optimal conditions including the neighboring factors for the desired frequency are required to implement the system with tunable impedance matching circuits.

The tunability of adaptive impedance matching modules is controlled by the following: the L network [19,20] consisting of a series LC and a parallel LC network; the capacitance array [21–25] configured by parallel switched capacitors; and the tuning transformer [26] based on the nonlinear properties of the ferromagnetic core material. However, these circuits have intolerably high loss and are not suitable for portable communication devices. Therefore, low loss tunable matching circuit would be useful for many applications, especially, for portable wireless communication devices.

In this paper, in order to improve system performance such as extended reading range and high efficiency in power transfer, a simple tunable antenna with switchable impedance matching networks operating at a specific distance is presented.

## 2. SWITCHABLE IMPEDANCE MATCHING NETWORKS

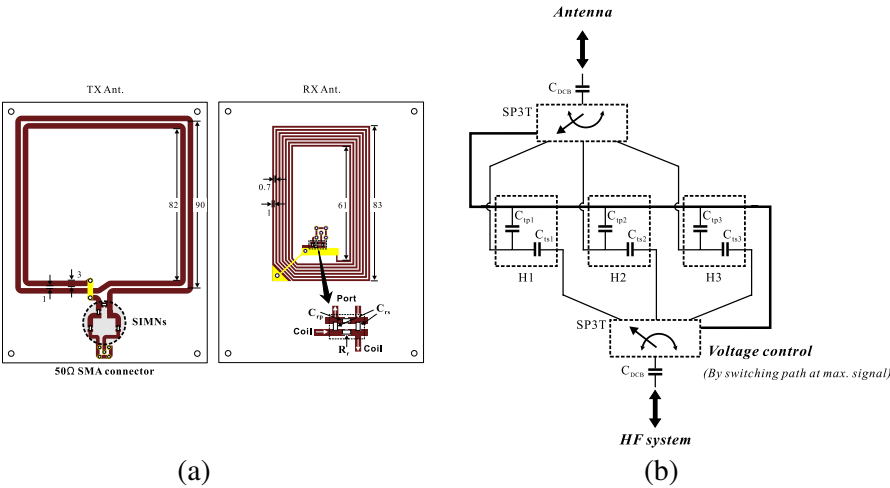
In this section, the proposed switchable impedance matching networks that operate at a specific distance between the transmitting and receiving antennas are discussed. After introducing the configuration and operating principles of the proposed matching networks, the equivalent circuit analysis of the proposed matching networks has been carried out.

2.1. Operating Principle

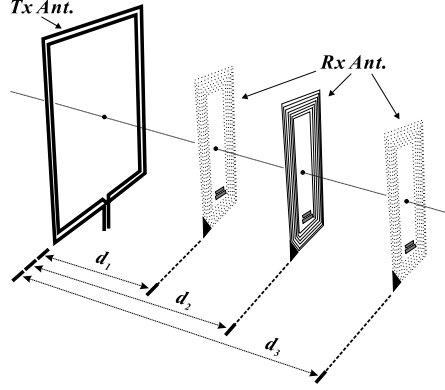
In NFC using the inductive coupling, besides magnetic field, the mutual inductance and the coupling factor between two devices are important parameters since the system performance is related to the function of distances between the transmitting and receiving antennas. As the value of coupling factor related to the antenna distance is increased, the resonant frequency splits resulting in the degradation of  $S_{21}$  magnitude due to the impedance mismatch [14].

Figure 1 shows the overall block diagram of an antenna system with the proposed impedance matching networks consisting of single-pole triple-throw (SP3T) switches and capacitors. The configuration of the proposed impedance matching networks, such as H1, H2, and H3, can be designed by series and shunt capacitors. At the specific distance ( $d_1$ ,  $d_2$ ,  $d_3$ ) between the transmitting and receiving antennas, in order to reduce the impedance mismatch, the capacitances of the proposed matching networks are determined.

As shown in Fig. 2, the arrangement between transmitting and receiving antennas is depicted according to the distance of  $d_1$ ,  $d_2$ , and  $d_3$ . As the receiving antenna in the concentric axis approaches the transmitting antenna, the mutual inductance increases and causes the antenna mismatch. As a result, the power efficiency or the reading



**Figure 1.** (a) Geometry of the designed antenna system with switchable impedance matching networks in the transmitting and receiving antennas. (b) Overall blocks of the switchable impedance matching networks which consist of SP3T switches and capacitors. H1, H2, and H3 are the impedance matching networks operating a specific distance between the transmitting and receiving antennas.



**Figure 2.** Arrangement between transmitting and receiving antennas having the distances of  $d_1$ ,  $d_2$ , and  $d_3$ .

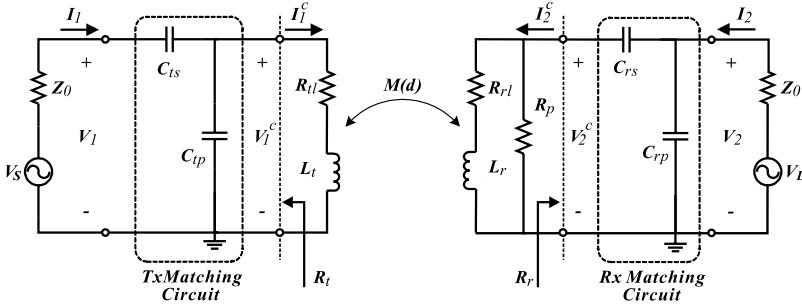


**Figure 3.** Equivalent circuit model for the proposed antenna with an impedance matching network in any distance.

range is drastically reduced. In case of the high  $Q$  systems with limited bandwidth, this phenomenon is observed even more clearly. To solve this problem, we present an effective matching technique by switching the determined impedance matching networks according to the matching distances. The proposed technique does not require automatic matching algorithm and various matching networks but has high power efficiency within the operating distance because of the proposed matching networks.

## 2.2. Equivalent Circuit Analysis

This work concentrates on the system using the 13.56 MHz frequency band for HF RFID and NFC applications that are currently aimed for

mobile phones. The configuration of the transmitting and receiving antennas is depicted in Fig. 1. The proposed matching networks are simply modeled by the equivalent circuit model in Fig. 3. The transmitting and receiving antennas are modeled by series resistors ( $R_{tl}$ ,  $R_{rl}$ ) and inductors ( $L_t$ ,  $L_r$ ), respectively. Impedance matching circuit is implemented by series and shunt capacitors. By inserting the additional shunt resistor ( $R_p$ ) in the receiving antenna, it makes the quality factor lower, and increases the bandwidth of system, resulting in a higher possible transmission rate. Both the input and output impedances are considered to be  $Z_0$ ,  $50\Omega$ .

The mutual inductance between two loops with a single turn is given by the double integral Neumann formula (1):

$$M_{12} = \frac{\psi_2}{I_1} = \frac{\mu_0}{4\pi} \oint_{c_1} \oint_{c_2} \frac{dl_1 \cdot dl_2}{r_{12}}, \quad (1)$$

where  $\mu_0$  is the magnetic constant ( $4\pi \times 10^{-7}$  H/m);  $c_1$  and  $c_2$  are the curves spanned by the loops;  $r_{12}$  is the distance between two points.

Based on the simultaneous conjugate matching (SCM) condition at a certain distance ( $d$ ) between two antennas, the simultaneously matched transfer efficiency ( $|S_{21}|^2$ ) and loaded  $Q$  at  $x$  cm are calculated by the Thevenin equivalent circuit and the definition of the  $S$  parameter.  $V_1$ ,  $V_2$ ,  $I_1$ , and  $I_2$  as shown in Fig. 3 can be expressed as

$$\begin{aligned} V_1 &= V_1^C - jX_{ts}I_1 & I_1 &= I_1^C - \frac{V_1^C}{jX_{tp}} \\ V_2 &= V_2^C - jX_{rs}I_2^C & I_2 &= I_2^C - \frac{V_2}{jX_{rp}}. \end{aligned} \quad (2)$$

As shown in Fig. 3,  $V_1^C$  and  $V_2^C$  must be satisfied with

$$\begin{aligned} V_1^C &= (R'_{tl} + jX_{tl})I_1^C - (R_M + jX_M)I_2^C \\ V_2^C &= -(R_M + jX_M)I_1^C + (R'_{rl} + jX_{rl})I_2^C, \end{aligned} \quad (3)$$

in which

$$\begin{aligned} R'_{tl} &= R_{tl} + \frac{X_M^2}{R_p} \\ R'_{rl} &= R_{rl} + \frac{X_M^2}{R_p} \\ R_M &= \frac{X_M X_{rl}}{R_p}. \end{aligned} \quad (4)$$

In the case of the SCM condition at  $d$  cm in the operating frequency ( $f_0$ , 13.56 MHz),  $S_{11}$  and  $S_{22}$  should be set to zero.

Equivalent resistance,  $R_{t,d,f_0}$  and  $R_{r,d,f_0}$ , toward the source and load from antennas can be simplified as (5), respectively:

$$\begin{aligned} R_{t,d,f_0} &\approx R'_{tl,d,f_0} \sqrt{1 + Q'^2_{M,d,f_0}} \\ R_{r,d,f_0} &\approx R'_{rl,f_0} \sqrt{1 + Q'^2_{M,d,f_0}}, \end{aligned} \quad (5)$$

where

$$Q'_{M,d,f_0} = \frac{X_{M,d,f_0}}{\sqrt{R'_{tl,d,f_0} R'_{rl,f_0}}}. \quad (6)$$

The  $(|S_{21}|^2_{x,f_0})$  at  $d$  cm distance with the SCM conditions at  $f_0$  can be derived as

$$|S_{21}|^2_{x,f_0} = \frac{1 + X^{(x,d)}_{M,f_0}}{\left( \sqrt{1 + Q'^{-2}_{M,d,f_0}} + \sqrt{Q'^{-2}_{M,d,f_0}} + \frac{1}{2} \frac{X^{(x,d)}_{M,f_0}}{\sqrt{1 + Q'^{-2}_{M,d,f_0}}} \right)^2}, \quad (7)$$

where

$$X^{(x,d)}_{M,f_0} = \frac{X^2_{M,x,f_0} - X^2_{M,d,f_0}}{X^2_{M,d,f_0}}. \quad (8)$$

At matching distances such as  $d_1$ ,  $d_2$ , and  $d_3$  cm, (7) can be simplified to (9). It means that  $|S_{21}|^2$  (transfer efficiency) reaches 100% if the reactance due to the mutual inductance increases to infinity. On the other hand, the transfer efficiency in the distance away from the matching distance is reduced as shown in (7) due to the mutual inductance.

$$|S_{21}|^2_{d,f_0} \approx \frac{1}{\left( \sqrt{1 + Q'^{-2}_{M,d,f_0}} + \sqrt{Q'^{-2}_{M,d,f_0}} \right)^2}. \quad (9)$$

The loaded  $Q$  between two devices can be calculated by analyzing the  $S_{21}$  characteristic with regard to the frequency. After searching for the 3 dB bandwidth from the  $|S_{21}|^2_{x,d,f}$ , which can be obtained from the  $S$  parameter definition, the  $Q_{loaded}$  can be determined by the resonant frequency over 3 dB bandwidth in (10) if  $Q'_{M,d,f_0}$  is much larger than 1. This leads to a decrease in the  $Q_{loaded}$  because the mutual inductance

increases and vice-versa.

$$Q_{loaded} \approx \begin{cases} \frac{\sqrt{Q'_{tl,d,f_0} Q'_{rl,f_0}}}{\sqrt{2} \sqrt{Q'^2_{M,d,f_0}} \left(1 + \frac{Q'^{-2}_{M,d,f_0}}{4}\right)} & \text{if } Q'_{M,d,f_0} \gg 1 \\ \frac{\sqrt{Q'_{tl,d,f_0} Q'_{rl,f_0}}}{1.29 \left(1 + 0.55 Q'^2_{M,d,f_0}\right)} & \text{if } Q'_{M,d,f_0} \ll 1, \end{cases} \quad (10)$$

where

$$Q'_{tl,d,f_0} = \frac{X_{tl,f_0}}{R'_{tl,d,f_0}}, \quad Q'_{rl,f_0} = \frac{X_{rl,f_0}}{R'_{rl,f_0}}. \quad (11)$$

In a practical case, the receiving antenna has been matched regardless of the transmitting antenna. The transmitting antenna has the proposed matching networks within the operating range. In this case, (5) is changed by

$$R'_{t,d,f_0} \approx R'_{tl,d,f_0} + \frac{X^2_{M,d,f_0}}{2R'_{rl,f_0}} \quad (12)$$

$$R'_{r,d,f_0} \approx R'_{rl,f_0}.$$

Also, the transfer efficiency in (7) and (9) can be given by (13) and (14), respectively.

$$|S_{21}|^2_{x,f_0} = \frac{1 + X^{(x,d)}_{M,f_0}}{2 \left(1 + \frac{2}{Q'^2_{M,d,f_0}}\right) \left[1 + \frac{1}{2} \left(1 + \frac{2}{Q'^2_{M,d,f_0}}\right)^{-1} X^{(x,d)}_{M,f_0}\right]^2}. \quad (13)$$

$$|S_{21}|^2_{d,f_0} \approx \frac{1}{2 \left(1 + \frac{2}{Q'^2_{M,d,f_0}}\right)}. \quad (14)$$

From (14), the maximum transfer efficiency ( $|S_{21}|^2$ ) is  $-3$  dB although the mutual inductance approaches to infinity.

The  $Q'_{loaded}$  using the transmitting antenna with the proposed

**Table 1.** Antenna parameters of equivalent circuit models.

Antenna	Parameter	Value
TX	$R_t$	$0.38 \Omega$
	$L_t$	$1.01 \mu\text{H}$
	$unloaded Q_t$	226
RX	$R_r$	$2.34 \Omega$
	$R_p$	$20 \text{ k}\Omega$
	$L_r$	$5.30 \mu\text{H}$
	$unloaded Q_r$	36

matching networks can be simplified to

$$Q'_{loaded} \approx \begin{cases} \frac{\sqrt{Q'_{tl,d,f_0} Q'_{rl,f_0}}}{4 \left( 1 + \frac{2}{Q'^2_{M,d,f_0}} - \frac{48}{Q'^4_{M,d,f_0}} \right)} & \text{if } Q'_{M,d,f_0} \gg 1 \\ \frac{\sqrt{Q'_{tl,d,f_0} Q'_{rl,f_0}}}{1.29 \left( 1 + 0.43 Q'^2_{M,d,f_0} \right)} & \text{if } Q'_{M,d,f_0} \ll 1. \end{cases} \quad (15)$$

### 3. PRACTICAL DESIGN AND EXPERIMENTAL RESULTS

Figure 1(a) shows the transmitting antenna designed by using the proposed matching networks, whereas the receiving antenna follows the inlay model of the TI Tag-it HF-I Transponder [27]. In order to enhance the reproducibility, the proposed design is implemented by a printed circuit board (PCB) using an FR4 substrate with 1 mm thickness. Using a vector network analyzer, the physical antenna parameters of the equivalent circuit models are measured in Table 1. The unloaded  $Q$  factors of the transmitting and receiving antennas are calculated by their equivalent circuits, the series  $R$  and  $L$ .

Table 2 shows the component values of the proposed matching networks at prearranged matching distances of  $d_1$  (3 cm),  $d_1$  (6 cm), and  $d_3$  (9 cm). For the receiving antenna having the fixed value of matching circuit ( $C_{rs}$  and  $C_{rp}$ ), the antenna impedance is  $50 \Omega$  matched at the operating frequency of 13.56 MHz. In order to have a maximum transfer efficiency between the transmitting and receiving antennas



**Table 2.** Component values of the proposed networks at a matching distance.

Antenna	Matching distance (cm)	Elements	Value (pF)	
			Calculated	Designed
TX	$d_1 = 3$	$C_{ts,1}$	105	121
		$C_{tp,1}$	38	43
	$d_2 = 6$	$C_{ts,2}$	40.5	43
		$C_{tp,2}$	97	102
	$d_3 = 9$	$C_{ts,3}$	21.9	20.3
		$C_{tp,3}$	114.7	124
RX	-	$C_{rs}$	54	47
		$C_{rp}$	406	300

in (13), the proposed matching networks ( $C_{ts,i}|_{i=1\sim3}$  and  $C_{tp,i}|_{i=1\sim3}$ ) of the transmitting antenna are determined at  $d_1$ ,  $d_2$ , and  $d_3$ . The transmitting system using the proposed matching networks searches for the maximum value from the received signal by switching the three channel impedance matching networks.

Based on the SCM condition of the transmitting and receiving antennas in Section 2, the  $S_{21}$  (related to the efficiency) can be depicted as shown in Fig. 4(a). According to the matching distance, the maximum value of the expected  $S_{21}$  decreases due to the degradation of the mutual inductance. However, by reducing the equivalent series resistances ( $R_t$  and  $R_r$ ) or by increasing the quality factor for the transmitting and receiving antennas, the expected  $S_{21}$  can be improved. On the other hand, the maximum difference of the expected  $S_{21}$  is approximately 8 dB within the operating range (0 cm–12 cm) and causes significant damage to the receiving system since it is about six times higher than an induced voltage level.

As shown in Fig. 4(b), the expected loaded  $Q$  in SCM conditions is proportional to the loop distance and is lower in close vicinity to the transmitting antenna. That is, a wide impedance bandwidth for robust and reliable communication can be achieved.

Using Table 2, the expected  $S_{21}$  and loaded  $Q$  is calculated as shown in Fig. 5(a) and Fig. 5(b), respectively. Due to the detuning effect in the receiving antenna,  $S_{21}$  and  $Q$  are nearly uniform within the operating range. In Table 3, we summarize the comparison of the FM conditions having a 3 cm matching distance, SCM conditions,

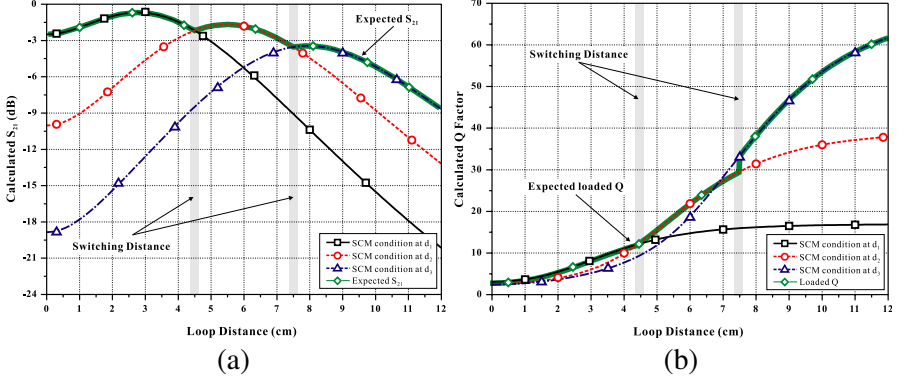


**Figure 4.** Calculated (a)  $S_{21}$  and loaded  $Q$ , (b) for the SCM conditions.

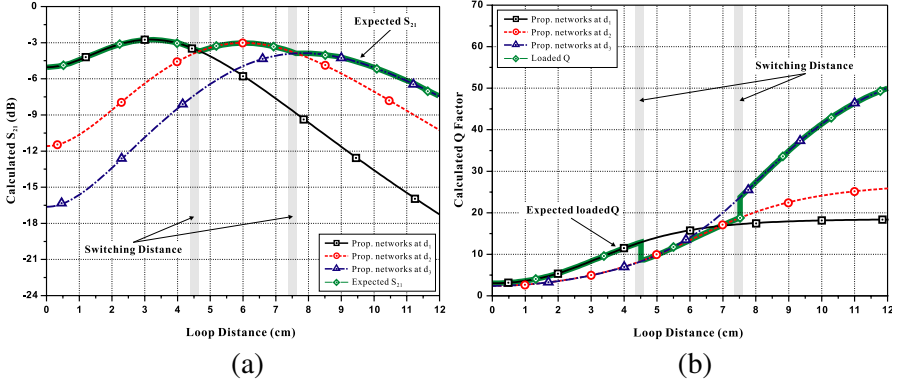


**Figure 5.** Calculated (a)  $S_{21}$  and loaded  $Q$ , (b) for the proposed networks.

**Table 3.** Comparison to the  $S_{21}$  between the matching scheme against the matching distance.

Distance (cm)	FM conditions (dB)	SCM conditions (dB)	Proposed networks (dB)
3	-2.76	-0.72	-2.76
6	-5.88	-1.81	-3.02
9	-11.8	-3.94	-4.25

and the proposed networks in terms of the  $S_{21}$  in the transmitting and receiving antennas. The maximum difference of the proposed networks is less than 1.5 dB within the matching distance.

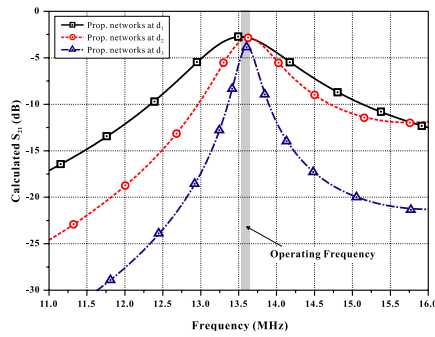
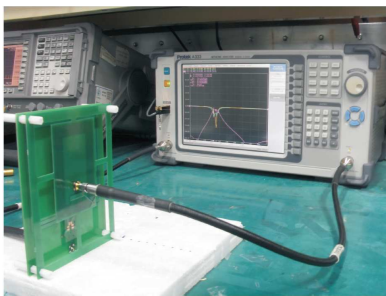
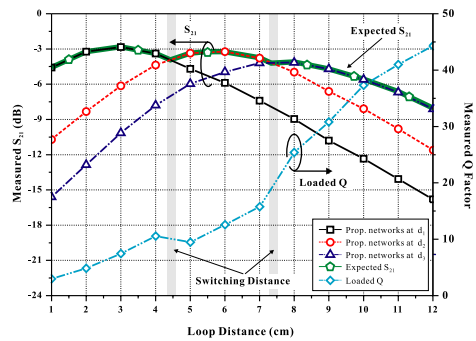


**Figure 6.** Calculated  $S_{21}$  as a function of frequency for the proposed networks given the values in Table 2.



(a)



(b)

**Figure 7.** (a) Measurement of  $S_{21}$  between transmitting and receiving antennas in any distance using a vector network analyzer. (b) Expected  $S_{21}$  and loaded  $Q$  for the matching distance in the measurements.

The  $S_{21}$  corresponding to frequencies is depicted in Fig. 6. From the 3 dB bandwidth, the tighter the spacing between the transmitting and receiving antennas, the lower  $Q$  is obtained.

As shown in Fig. 7(a),  $S_{21}$  is measured by fixing the distance and using a vector network analyzer. Fig. 7(b) shows the expected  $S_{21}$  and loaded  $Q$  for the matching distance in the measurements. In order to avoid the distance error between the transmitting and receiving antennas, the measurement is performed at the intervals of 1 cm. An excellent agreement between the calculated and measured data in Fig. 8 is obtained in the strongly coupled region. However, in the loosely coupled region where the distance is larger than the loop radius, the  $Q$  of the measured data is lower than that of the calculated data because a parasitic capacitor in the receiving antenna lowers the additional shunt resistor ( $R_p$ ).

In order to compare the power transfer efficiency between the FM condition at  $d_1$  and the proposed networks, voltage levels receiving from the transmitting antenna are measured. The transmitting antenna is connected to the signal generator with a 30 mWatt magnitude and

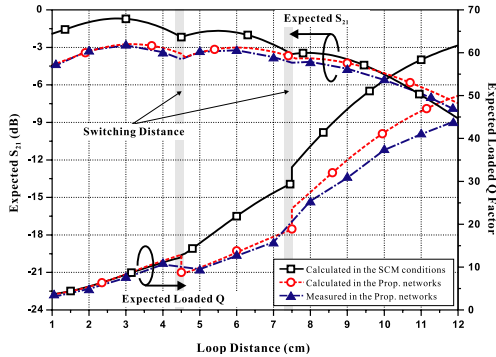


**Figure 8.** Comparison to the expected  $S_{21}$  and loaded  $Q$  for the SCM conditions and proposed networks between the calculated and measured results.

**Table 4.** Voltage levels and normalized results receiving from the transmitting antenna.

Distance (cm)	Voltage Levels (V)		Normalized Results*	
	FM at $d_1$	Prop. networks	FM at $d_1$	Prop. networks
1	2.42	2.42	0.90	0.90
2	2.67	2.67	0.99	0.99
3	2.70	2.70	1.00	1.00
4	2.48	2.66	0.92	0.99
5	2.00	2.75	0.74	1.02
6	1.66	2.62	0.61	0.97
7	1.38	2.50	0.51	0.93
8	1.07	2.46	0.40	0.91
9	0.88	2.32	0.33	0.86
10	0.70	2.03	0.26	0.75
11	0.57	1.71	0.21	0.63
12	0.51	1.54	0.19	0.57

\* Based on the voltage level with a FM condition at  $d_1$  (3 cm).

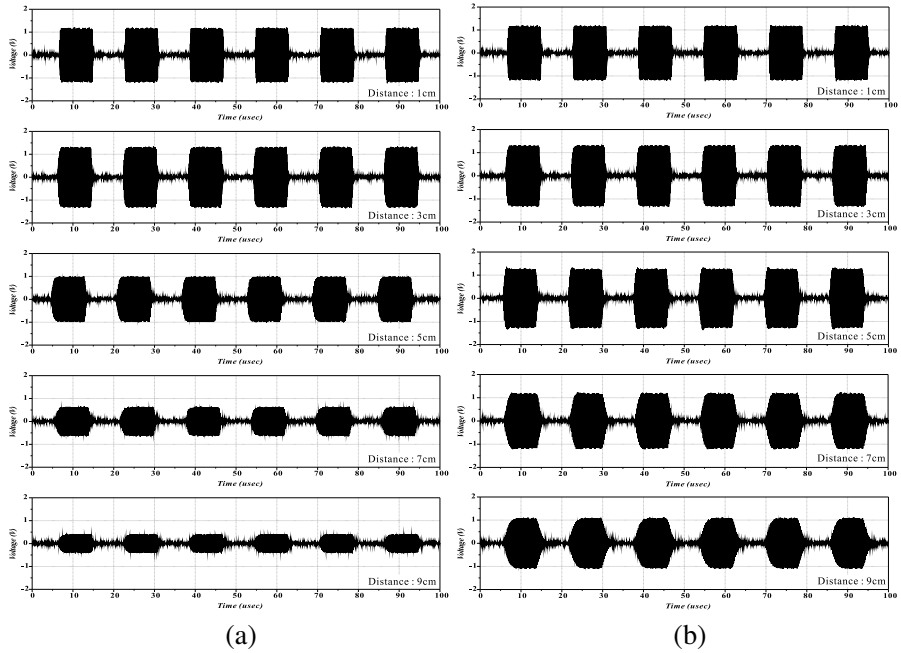


**Figure 9.** The signal waveforms of (a) the power transmission from the transmitting antenna with a FM condition and (b) the proposed networks.

pulse modulation (pulse period =  $16\mu\text{s}$ , pulse width =  $8\mu\text{s}$ ) at 13.56 MHz.

The signal waveforms of the receiving antenna are measured using an oscilloscope. The voltage levels with regard to each distance can be obtained as shown in Table 4. In case of a power transmission having a FM condition at  $d_1$ , voltage levels are gradually decreased within the operating distance. However, voltage levels at proposed networks are unfading by controlling the impedance matching networks with regard to the distance. Figs. 9(a) and 9(b) illustrate the voltage levels obtained from the receiving antenna according to the transmitting antenna with a FM condition or the proposed networks. If the received powers with a FM condition at 3cm normalize those of the proposed networks, a power transfer efficiency rating of 89% results at 12 cm in the proposed networks.

#### 4. CONCLUSION

In this paper, switchable distance-based impedance matching networks for a tunable high frequency system is presented, which improve system

performance by switching the predetermined impedance matching networks in the operating range, regardless of automatic control algorithms and complicated matching networks. Easy tunability is achieved simply by checking the received signal level of the three channel impedance matching networks. Moreover, NFC and RFID systems require uniform  $S_{21}$  characteristics in order to prevent the excessive voltage of the transponder IC when further increasing the coupling factor and to use wide bandwidth in communications. This means that the  $Q$  of these systems must be kept low. The proposed design technique offers low  $Q$  and uniform  $S_{21}$  characteristics through the proper selection of impedance matching networks. In the operating range (0 cm–12 cm), it is less than 5 dB variation of  $S_{21}$ , and provides improved efficiency of a maximum of 89%. Due to the attractive characteristics of the proposed networks, the proposed technique can ensure more reliable and robust system designs for wireless power transfer and data communications.

## REFERENCES

1. Rappaport, T. S., "Wireless personal communications: Trends and challenges," *IEEE Antennas and Propagation Magazine*, Vol. 33, No. 5, 19–29, Oct. 1991.
2. Ou Yang, J., J. Zhang, K. Zhang, and F. Yang, "Compact folded dual-band slot antenna for wireless communication USB dongle application," *Journal of Electromagnetic Waves and Applications*, Vol. 25, No. 8–9, 1221–1230, 2011.
3. Li, J.-F. and Q.-X. Chu, "A compact dual-band MIMO antenna of mobile phone," *Journal of Electromagnetic Waves and Applications*, Vol. 25, No. 11–12, 1577–1586, 2011.
4. Xie, K., Y.-M. Liu, H.-L. Zhang, and L.-Z. Fu, "Harvest the ambient AM broadcast radio energy for wireless sensors," *Journal of Electromagnetic Waves and Applications*, Vol. 25, No. 14–15, 2054–2065, 2011.
5. Lin, D.-B., P.-C. Tsai, I.-T. Tang, and W.-S. Chiu, "Planar inverted-L antenna for octa-band operations of smart handsets," *Journal of Electromagnetic Waves and Applications*, Vol. 25, No. 16, 2188–2200, 2011.
6. Tak, Y., J. Park, and S. Nam, "Mode-based estimation of 3 dB bandwidth for near-field communication systems," *IEEE Transactions on Antennas and Propagation*, Vol. 59, No. 8, 3131–3135, Aug. 2011.

7. Jiang, B., J. R. Smith, M. Philipose, S. Roy, K. Sundara-Rajan, and A. V. Mamishev, "Energy scavenging for inductively coupled passive rfid systems," *IEEE Transactions on Instrumentation and Measurement*, Vol. 56, No. 1, 118–125, Feb. 2007.
8. Imura, T. and Y. Hori, "Maximizing air gap and efficiency of magnetic resonant coupling for wireless power transfer using equivalent circuit and Neumann formula," *IEEE Transactions on Industrial Electronics*, Vol. 58, No. 10, 4746–4752, Oct. 2011.
9. Witschnig, H., M. Roland, M. Gossar, and H. Enzinger, "Parameter characterisation and automatic impedance matching of 13.56 MHz NFC antennas," *Elektrotechnik und Informationstechnik, SpringerLink*, Vol. 126, No. 11, 415–422, Nov. 2009.
10. Kurs, A., A. Karalis, R. Moffatt, J. D. Joannopoulos, P. Fisher, and M. Soljacic, "Wireless power transfer via strongly coupled magnetic resonances," *Science*, Vol. 317, No. 5834, 83–86, Jul. 2007.
11. Peng, L., O. Breinbjerg, N. A. Mortensen, "Wireless energy transfer through non-resonant magnetic coupling," *Journal of Electromagnetic Waves and Applications*, Vol. 24, No. 11–12, 1587–1598, 2010.
12. Peng, L., J. Y. Wang, L.-X. Ran, O. Breinbjerg, and N. A. Mortensen, "Performance analysis and experimental verification of mid-range wireless energy transfer through nonresonant magnetic coupling," *Journal of Electromagnetic Waves and Applications*, Vol. 25, No. 5–6, 845–855, 2011.
13. Jang, B.-J., S. Lee, and H. Yoon, "HF-band wireless power transfer system: Concept, issues, and design," *Progress In Electromagnetics Research*, Vol. 124, 211–231, Jan. 2012.
14. Sample, A. P., D. A. Meyer, and J. R. Smith, "Analysis, experimental results, and range adaptation of magnetically coupled resonators for wireless power transfer," *IEEE Transactions on Industrial Electronics*, Vol. 58, No. 2, 544–554, Feb. 2011.
15. Choi, J. and C. Seo, "High-efficiency wireless energy transmission using magnetic resonance based on metamaterial with relative permeability equal to  $-1$ ," *Progress In Electromagnetics Research*, Vol. 106, 33–47, Jul. 2010.
16. Liu, Y., Y. J. Zhao, and Y. G. Zhou, "Lumped dual-frequency impedance transformers for frequency-dependent complex loads," *Progress In Electromagnetic Research*, Vol. 126, 121–138, Mar. 2012.
17. Sun, Y. and W. K. Lau, "Evolutionary tuning method for automatic impedance matching in communication systems," 1998

- IEEE International Conference on Electronics, Circuits and Systems*, 73–77, 1998.
18. Gu, Q., J. R. de Luis, A. S. Morris, and J. Hilbert, “An analytical algorithm for pi-network impedance tunners,” *IEEE Transactions on Circuits and System-I: Regular Papers*, 2894–2905, Dec. 2011.
  19. Van Bezooijen, A., M. A. de Jongh, F. van Straten, R. Mahmoudi, and A. van Roermund, “Adaptive impedance-matching techniques for controlling L networks,” *IEEE Transactions on Circuits and Systems-I: Regular Papers*, Vol. 57, No. 2, 495–505, Feb. 2010.
  20. Jang, T., S. Lim, and T. Itoh, “Tunable compact asymmetric coplanar waveguide zeroth-order resonant antenna,” *Journal of Electromagnetic Waves and Applications*, Vol. 25, No. 17–18, 2379–2388, 2011.
  21. Sanchez, C., J. de Mingo, L. Saenz, P. Garcia, P. L. Carro, and A. Valdovinos, “Performance evaluation of an automatic impedance synthesizer based on RF switches,” *IEEE 69th Vehicular Technology Conference, 2009. VTC Spring 2009*, 1–5, 2009.
  22. Liang, Y., C. W. Domier, and N. C. Luhmann, Jr., “RF MEMS extended tuning range varactor and varactor based true time delay line design,” *PIERS Online*, Vol. 4, No. 4, 433–436, 2008.
  23. Ourir, A., R. Abdeddaim, and J. de Rosny, “Tunable trapped mode in symmetric resonator designed for metamaterials,” *Progress In Electromagnetics Research*, Vol. 101, 115–123, 2010.
  24. Chan, F., W. Po, E. de Foucauld, D. Morche, P. Vincent, and E. Kerherve, “A novel method for synthesizing an automatic matching network and its control unit,” *IEEE Transactions on Circuits and Systems-I: Regular Papers*, Vol. 58, No. 9, 2225–2236, Sep. 2011.
  25. De Mingo, J., A. Valdovinos, A. Crespo, D. Navarro, and P. Garcia, “An RF electronically controlled impedance tuning network design and its application to an antenna input impedance automatic matching system,” *IEEE Transactions on Microwave Theory and Techniques*, Vol. 52, No. 2, 489–497, Feb. 2004.
  26. Wegleiter, H., B. Schweighofer, C. Deinhammer, G. Holler, and P. Fulmek, “Automatic antenna tuning unit to improve RFID system performance,” *IEEE Transactions on Instrumentation and Measurement*, Vol. 60, No. 8, 2797–2803, Aug. 2011.
  27. Instruments, T., “Tag-it HF-I standard transponder inlays large rectangle,” *TI-RFID*, Dec. 2005.